Long vs short-term synaptic learning rules after optogenetic spike-timing-dependent plasticity

Margarita Anisimova, Bas van Bommel, J. Simon Wiegert, Marina Mikhaylova, Thomas G. Oertner[1], Christine E. Gee[1]*

Center for Molecular Neurobiology Hamburg, University Medical Center Hamburg-Eppendorf, Hamburg, Germany

[1]these authors contributed equally to this work

*correspondence:

Dr. Christine E. Gee
Institute for Synaptic Physiology
Center for Molecular Neurobiology Hamburg
Falkenried 94
20251 Hamburg
Germany

christine.gee@zmnh.uni-hamburg.de

+49 40 7410 57190

Abstract

Spike-timing-dependent plasticity (STDP) is a candidate mechanism for information storage in the brain. However, it has been practically impossible to assess the long-term consequences of STDP as recordings from postsynaptic neurons last at most one hour. We assessed both the short-term (20 minutes) and long-term (3 days) effects of optically-induced STDP (oSTDP) using two colors of light to independently activate CA3 and CA1 neurons expressing the opsins ChrimsonR and CheRiff. During patch-clamp recordings short-term effects followed classic STDP rules, synapses potentiated when postsynaptic spikes followed presynaptic spikes (tLTP, causal pairing) and depressed when postsynaptic spikes were first (tLTD, anti-causal pairing). Surprisingly, three days after inducing oSTDP without patching the neurons, tLTP was evident regardless of pairing sequence. Potentiation depended on NMDA receptors and spontaneous activity was necessary in the two days following oSTDP. Our data suggest that tLTD at Schaffer collateral synapses is a transitory phenomenon or a recording artifact.

Introduction

Synaptic strength changes after coincident activity in the pre- and postsynaptic neurons, a process commonly referred to as spike-timing-dependent plasticity (STDP)[1]. In classical STDP, timing-dependent long-term potentiation (tLTP) is induced when synaptic responses precede postsynaptic action potentials, i.e. causal or Hebbian pairing. In contrast, timing-dependent long-term depression (tLTD) is induced when synaptic responses follow postsynaptic action potentials, i.e. anti-causal pairing[2–4]. While STDP is an attractive model for how memories may be formed[1,5–7], experiments are usually limited to 20-60 minutes, a time frame that is clearly not relevant for most forms of memory. This time limitation arises from the invasive nature of intracellular recordings, which are necessary to control postsynaptic spiking. We have followed individual CA1 pyramidal neuron spine synapses for a week after inducing LTP or LTD and observed that their stability is enhanced after LTP and decreases following LTD[8,9]. However, pairs of CA3-CA1 neurons may have multiple synaptic contacts and new connections may form, leaving what happens to the overall connection strength an open question we sought to answer.

The channelrhodopsins are ion channels that open in response to light, and since the discovery of channelrhodopsin-2[10] have been widely used to stimulate neurons with light in vitro and in vivo[e.g. 11–18]. In recent years, many channelrhodopsin variants have been discovered or engineered with varying kinetics, spectral sensitivities and ion selectivity[19–23]. We reasoned that using opsins with rapid kinetics and sensitive to different wavelengths of light, we could circumvent the need for intracellular/patch-clamp recordings and optically induce 'no-patch' STDP. Here, we present a two-color method to stimulate precisely timed action potentials in defined subsets of CA3 and CA1 pyramidal neurons for optogenetic induction of STDP (oSTDP). Whereas oSTDP induced classical tLTP and tLTD in short-term patch-clamp experiments, the outcome after 3 days was strong tLTP regardless of the activation sequence. Our findings support the conclusion that the short and long-term consequences of STDP are different.

Results

ChrimsonR and CheRiff are suitable for optogenetic STDP. To achieve our goal of independently spiking pre- and postsynaptic neurons, we reasoned that the red light sensitive ChrimsonR[20] and the blue/violet light-sensitive CheRiff[19] were the most promising pair of channelrhodopsins. ChrimsonR-tdTomato was expressed in a small subset of CA3 pyramidal neurons by local virus injection and several CA1 neurons were electroporated with DNA encoding CheRiff-eGFP (Fig. 1a). In order to visualize CheRiff-expressing CA1 neurons (hereafter referred to as CheRiff-CA1 neurons) without

activating them we also included DNA encoding mKate2 in our electroporation mix. We waited 7-10 days for expression of both channelrhodopsins before starting the experiments.

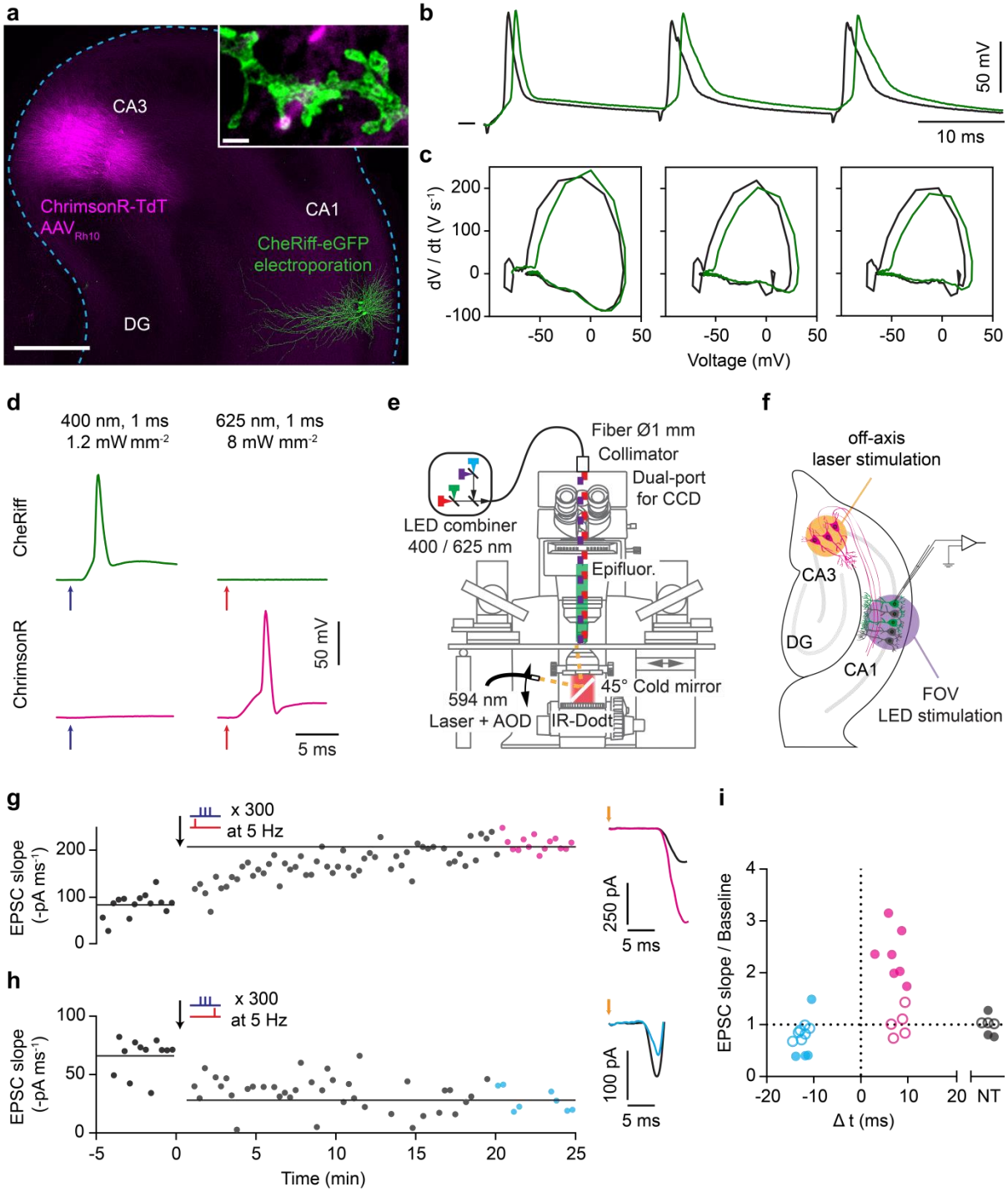

Fig. 1 | Optogenetic induction of spike-timing-dependent plasticity (oSTDP). a, Organotypic hippocampal slice culture, transfected with ChrimsonR and CheRiff to independently control spiking in CA3 and CA1 neurons, respectively. Insert: STED reconstruction of a Cheriff-CA1 oblique dendrite (green) and confocal image of presynaptic boutons (magenta) with a putative synaptic contact. Scale bars 500 µm, insert 1 µm. **b,** Action potentials (APs) induced by somatic current injection (black trace, 3 nA, 2 ms) or by optical stimulation (green trace, 405 nm, 1.2 mW mm^{-2}, 2 ms) of a CheRiff-CA1 pyramidal neuron. Electrical stimulation artefacts appear at 0, 20 and 40 ms. Black tick is at -80 mV. **c,** Phase plots of the corresponding APs from **b**. **d,** Example membrane responses of CheRiff-CA1 (upper traces) and ChrimsonR-CA3 (lower traces) expressing neurons to 405 nm (violet arrows) and 625 nm (red arrows) light. Note that 405 nm light evokes APs in the CheRiff

expressing neuron and only slight depolarization of the ChrimsonR-CA3 neuron. 625 nm light induced an AP in the ChrimsonR-CA3 neuron with no effect on the CheRiff-CA1 neuron. **e,** Diagram of the electrophysiological recording setup with on-axis LED and off-axis laser stimulation. **f,** Diagram of an organotypic hippocampal slice in the recording chamber. **g and h,** The slope of excitatory postsynaptic currents (EPSCs) recorded from CheRiff-CA1 neurons in response to laser stimulation of ChrimsonR-CA3 neurons at baseline and after oSTDP induction (arrows, t = 0). At right are the averaged EPSCs before (black points/trace) and after (magenta or cyan points/trace) oSTDP induction. **g,** Causal stimulation induced timing dependent potentiation ($n = 12$; $p < 0.0001$, magenta vs black, Kolmogorov-Smirnov). **h,** Anti-casual stimulation induced timing dependent depression ($n = 11$; $p = 0.0003$, cyan vs black, Kolmogorov-Smirnov). **i,** Average EPSC slope 20-25 minutes after oSTDP induction normalized to baseline from experiments as in **g** and **h**, Δt is the EPSP-spike timing interval during the pairing (c.f. Fig 2b). Hollow and filled points indicate individual experiments where EPSC slope did not or did change, respectively (Kolmogorov-Smirnov tests on raw values). NT, non-transfected neurons from slices subjected to causal light stimulation ($n = 7$).

Action potentials (APs) evoked by light stimulation of channelrhodopsin2 are prolonged relative to electrically-evoked APs[13]. As depolarization-induced increases in postsynaptic calcium are critical for plasticity, prolonged light-induced depolarization of the postsynaptic CA1 neurons would be expected to affect STDP[24,25]. We therefore compared electrically and light-evoked APs in CheRiff-CA1 pyramidal neurons (Fig. 1b, c). Importantly, using light to drive spiking in CheRiff-CA1 neurons did not greatly prolong AP depolarization relative to APs driven by current injection. The AP amplitude and half-widths were similar suggesting that driving APs with 405 nm light in CA1 neurons would not alter STDP timing rules.

As the threshold for light-induced APs is not only opsin dependent but also depends on expression levels and cell type, we performed a detailed analysis of the spectral sensitivity of ChrimsonR-CA3 and CheRiff-CA1 pyramidal neurons (Supplementary Fig. 1). According to this spectral analysis, we selected 405 nm (1.2 mW mm^{-2}) to activate CheRiff-CA1 neurons and 625 nm (8 mW mm^{-2}) to activate ChrimsonR-CA3 neurons which reliably and selectively spiked CA3 or CA1 pyramidal neurons using 2 ms flashes (Fig. 1c, Supplementary Fig. 1d). Although 405 nm light partially activates ChrimsonR, it did not spike ChrimsonR-CA3 neurons at 1 mW mm^{-2} (depolarization 0-3 mV, Fig. 1c, Supplementary Fig. 1b, d). Importantly, red light (625 nm) caused no photocurrents in CheRiff-CA1 neurons at intensities up to 100 mW mm^{-2} nor did the yellow epifluorescence light used to visualize mKate2 (Fig 1c, Supplementary Fig.1a). Thus, we never inadvertently depolarized the postsynaptic CheRiff-CA1 neurons (i.e. cultures were never exposed to light below 565 nm except during pairing).

oSTDP follows the short-term timing rules of classical STDP. We recorded baseline EPSCs in CheRiff- or non-transfected CA1 neurons (whole-cell voltage clamp at -70 mV) while optogenetically stimulating the ChrimsonR-CA3 neurons at 20 second intervals, by illuminating their somata with a condenser-coupled[26] orange (594 nm) laser (Fig. 1e and f). Condenser-coupled illumination was used as CA3 was outside the field of view of the objective when we patched the CA1 pyramidal neurons. After collecting the baseline for 5 minutes in voltage-clamp we switched to current-clamp mode. Single presynaptic spikes (300 orange/red flashes at 5 Hz, see methods) were paired with spike

84 bursts in the postsynaptic neuron (3 flashes at 50 Hz, 405 nm). Causal pairing, when the EPSP
85 preceded the first postsynaptic spike by about 10 ms, resulted in significant potentiation of EPSCs in
86 7 of 12 experiments (Fig. 1g and i). Anti-causal pairing, when postsynaptic spikes preceded EPSPs by
87 about 10 ms, significantly depressed EPSCs in 3 of 11 experiments (Fig. 1h and i). The outcomes after
88 causal and anti-causal pairing were significantly different ($p = 0.003$, Kolmogorov-Smirnov). The light
89 stimulation used for causal pairing had no overall effect in non-transfected neurons (median = 1.06,
90 Fig 1i), indicating that oSTDP was specific to CheRiff-CA1 neurons. Evidently, using light to induce
91 timed action potentials in pre- and postsynaptic neurons produces oSTDP with similar timing rules as
92 when action potentials are triggered by electrical stimulation[2,3,24,25,27–30].

93 **No-patch oSTDP induction in the incubator.** Having established conditions for inducing oSTDP, we
94 constructed illumination towers, each containing independently controlled, collimated, red (630 nm)
95 and violet (405 nm) high-power LEDs so that ChrimsonR and CheRiff-expressing neurons could be
96 stimulated in the incubator with defined light intensities (Fig. 2a). At the chosen intensities,
97 ChrimsonR and CheRiff-expressing neurons followed the 5 Hz stimulation pattern (single APs in CA3,
98 50 Hz triplets in CA1) with precise timing and high reliability (Fig. 2b, c). Non-transfected CA1 neurons
99 showed only EPSPs as expected (Fig. 2d).

100 Still, we were concerned about the specificity of postsynaptic activation. If synchronous activation of
101 ChrimsonR-CA3 neurons in the incubator directly drove CA1 neurons to fire APs, Hebbian plasticity
102 may be induced in all CA1 neurons and would no longer be contingent on light-induced spiking of the
103 CheRiff-CA1 neurons[31]. To test for potential burst firing of non-transfected neurons, we investigated
104 cFos activation patterns in cultures stimulated with the causal pairing protocol[32]. We found that
105 when the number of ChrimsonR-CA3 neurons in the slice was 53 or less, no cFos staining was seen in
106 CA1 neurons that were not expressing CheRiff (5/5 slices, 36-53 ChrimsonR-CA3 neurons). Given that
107 CheRiff-CA1 neurons were directly driven by the 405 nm light to burst fire, they did show cFos
108 staining (Fig. 2e). In 2 slices with 60-61 ChrimsonR-CA3 neurons, 7-10 untransfected CA1 neurons
109 showed cFos staining, indicating that CA3 stimulation at 5 Hz was directly driving some CA1 neurons
110 to burst fire. When the number of ChrimsonR-CA3 neurons increased to 96 or more, cFos staining
111 was evident throughout the entire CA1 (2/2 slices, not shown). In CA3, no cFos was detected in the
112 ChrimsonR-CA3 neurons driven with light at 5 Hz (Supplementary Fig. 2, 9/9 slices), but burst firing of
113 ChrimsonR-CA3 neurons, which was not part of our oSTDP protocols, did induce cFos in 39 ± 6% of
114 these neurons and in about the same number of non-transfected CA3 neurons (Supplementary Fig. 3,
115 6 slices). Thus, we aimed to transduce 20-30 ChrimsonR-CA3 neurons with a localized AAV injection
116 to avoid driving burst firing of postsynaptic CA1 neurons during oSTDP stimulation.

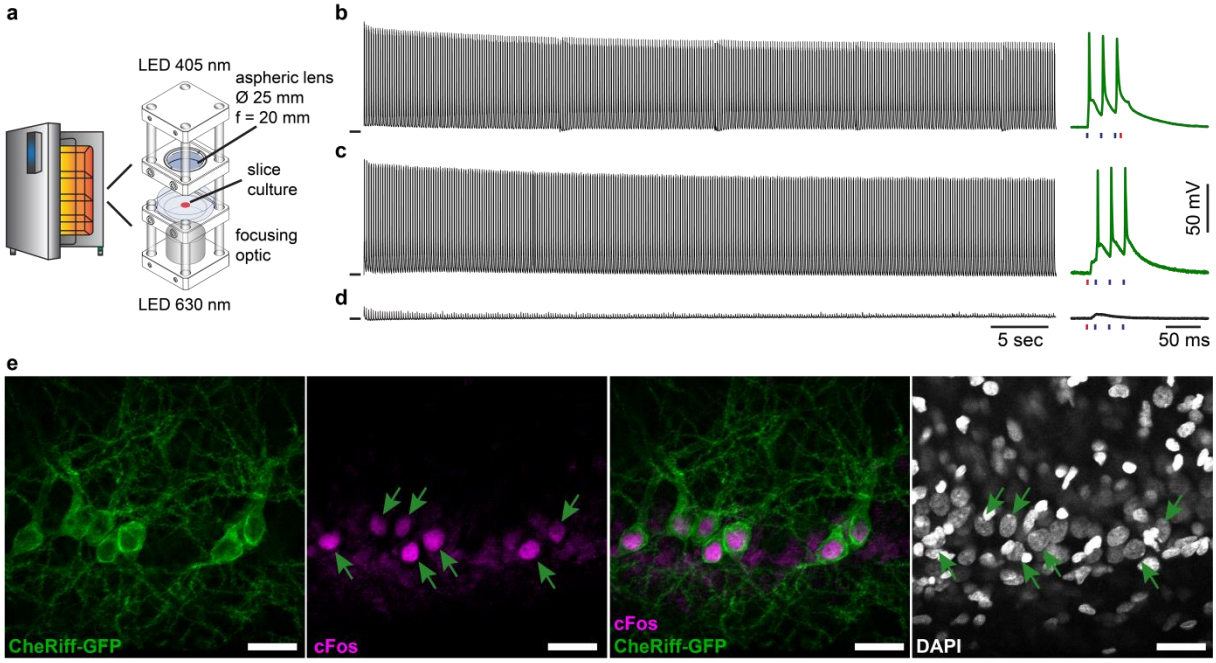

Fig. 2 | No-patch oSTDP stimulation induces cFos only in CheRiff CA1 neurons. a, Diagram of the device used for in-incubator optogenetic stimulation of ChrimsonR and CheRiff expressing neurons in hippocampal slice cultures. **b-d,** Membrane responses recorded from CA1 neurons during oSTDP induction: full recordings (left) and the responses to a single pairing (right). Black ticks are at -75 mV, red and violet ticks (right) indicate timing of light flashes. **b,** Firing pattern of a CheRiff-CA1 neuron during anti-causal pairing (-10 ms: 3 violet flashes at 50 Hz and 1 red flash 8 ms after, repeated 300x at 5 Hz). Note the EPSP following three action potentials. **c,** Same as **b**, but causal pairing (+10 ms: 1 red flash and 3 violet flashes at 50 Hz 12 ms after). Note the EPSP preceding three action potentials. **d,** Membrane voltage response of a non-transfected CA1 neuron during causal pairing. Note the EPSP and absence of action potentials. **e,** Expression of cFos in CA1 of a slice culture fixed 1.5 hours after causal in-incubator oSTDP stimulation. Confocal image stacks of CheRiff-CA1 neurons (green), anti-cFos (magenta) and overlay. At right are the DAPI stained nuclei. Green arrows point to nuclei of the CheRiff-CA1 neurons. Scale bars 50 µm

No difference in input strength 3 hours after no-patch oSTDP. In cultures that were not previously stimulated with light, we activated ChrimsonR-CA3 neurons with brief light pulses, sequentially recording EPSCs in several CA1 neurons (Fig. 3a, b). These recordings and all following were performed blind to the treatment group. The relative synaptic input strength onto the CheRiff-CA1 neurons was calculated by dividing the average EPSC slope, by the slope of the combined average EPSC recorded from at least 3 non-transfected neurons (Fig. 3c). The median input strength of CheRiff-CA1 neurons from cultures that were not previously stimulated with light was 0.91 (Fig. 3d, no pairing; mean = 1.04, CV = 0.53). Thus, in control conditions (without paired light stimulation) CheRiff-CA1 and neighboring CA1 neurons received equivalent input from the ChrimsonR-CA3 neurons. Somewhat surprisingly, when assessed about 3 hours after oSTDP induction, input strength was not significantly changed by either causal or anti-causal pairing, although a trend towards potentiation after causal pairing was apparent (Fig. 3d, -10 ms median = 1.04; +10 ms median = 1.62).

Input strength is potentiated three days after no-patch oSTDP. Three days after oSTDP causally-paired CheRiff-CA1 neurons received significantly stronger input (Fig. 3e, +10 ms: median = 2.13,

144 mean = 2.95, CV = 0.69). Interestingly, anti-causal pairing also resulted in stronger inputs (Fig. 3e, -10
145 ms: median = 1.8, mean = 2.51, CV = 0.89). The time interval between EPSPs and postsynaptic spikes
146 was important, as input strength did not change significantly when Δ*t* was +50 ms (Fig. 3e, +50 ms:
147 median = 0.97, mean = 2.44, CV = 1.18; -50 ms: median = 1.78, mean = 2.38, CV = 0.66). Coincident
148 activity of pre- and postsynaptic neurons was an absolute requirement for oSTDP as input strength
149 was unchanged 3 days after burst firing of the postsynaptic neurons alone (Fig. 3e, post only). We
150 found no differences between CheRiff- and non-transfected CA1 neurons in cellular parameters or
151 excitability (Supplementary Fig. 4). This strongly suggests that 3 days after oSTDP, tLTP was not due
152 to increased postsynaptic excitability[33–35]. Thus, oSTDP triggered lasting changes in relative input
153 strength that could be read-out 3 days later.

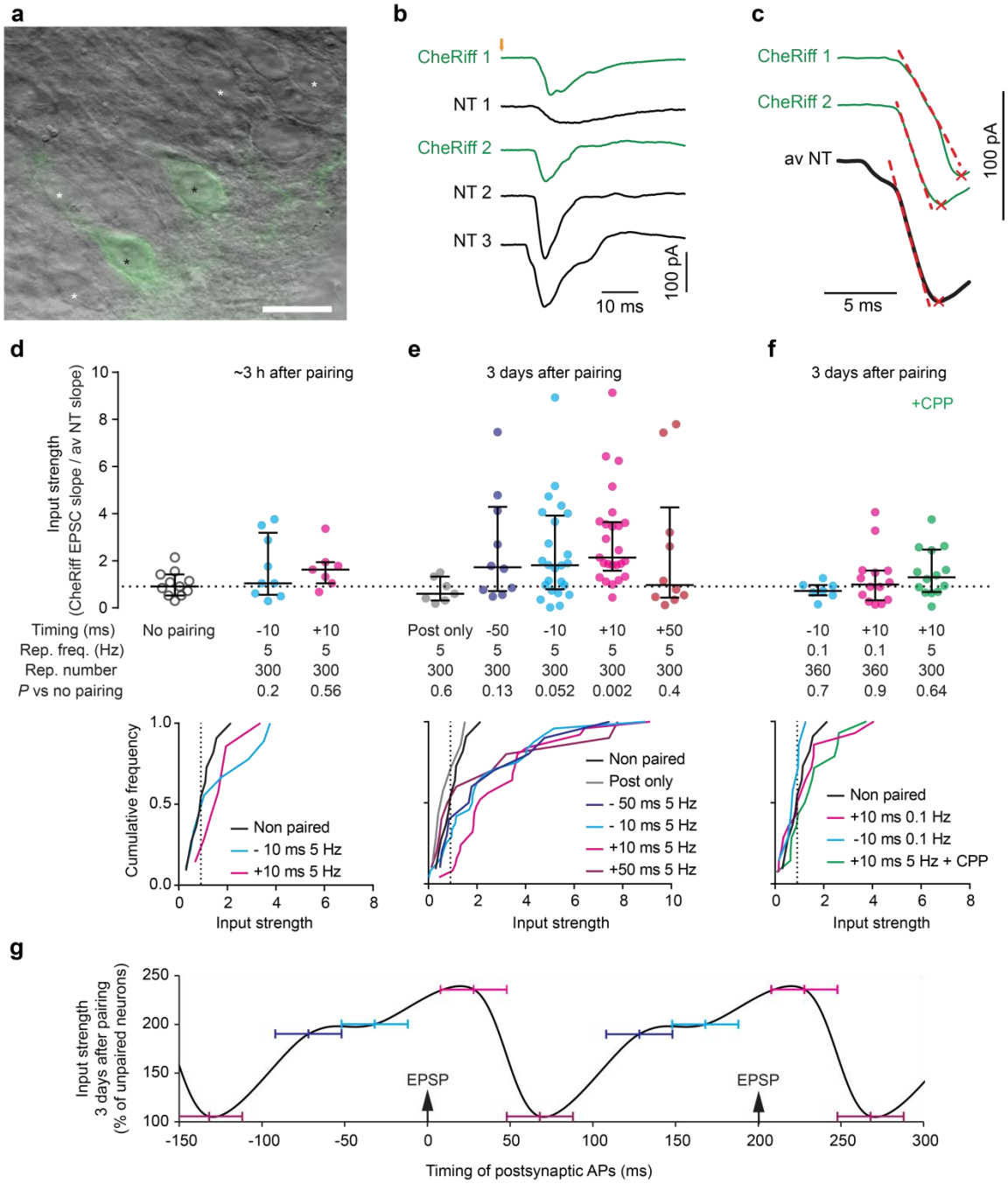

154

Fig. 3 | Three days after oSTDP only potentiation is evident. a, Dodt-contrast image (40x objective) of CA1 region with overlaid epifluorescence image. Black asterisks: CheRiff expressing pyramidal neurons; white asterisks: non-transfected pyramidal neurons, suitable for recording. Note that the actual field of view is about 30% larger. Scale bar 25 µm. **b,** Average EPSCs (10 sweeps), evoked by laser stimulation (arrow) of ChrimsonR-CA3 neurons. EPSCs were recorded sequentially from non-transfected (NT) and neighboring CheRiff-CA1 pyramidal neurons from a control (no pairing) slice as in **a**. **c,** Automatically-detected EPSC peak (red x) and slope (dashed red line, 20-60% peak). EPSCs from NT neurons were averaged before determining the NT slope. **d,** Normalized input strength of CheRiff-CA1 neurons recorded from control (no pairing) slices and slices ~3 hours after in-incubator oSTDP. Plotted are individual data points, median and 25-75% interquartile range and cumulative frequency distributions (below). The dotted line is the median input strength onto CheRiff-CA1 neurons of the non-paired slices (hollow grey points, n = 11). 'Timing' is the target interval between start of the EPSC and the first or last postsynaptic spike (-10 ms anti-causal pairing, n = 9; +10 ms causal pairing, n = 7). 'Rep. freq.' is the pairing repetition frequency. 'Rep. num.' is the number of pairings. **e,** As in **d** except 3 days after pairing. Post only: only violet light flashes (n's left to right = 7, 10, 24, 25, 10). **f,** As in **d** except the repetition frequency was reduced to 0.1 Hz (n's left to right = 7, 14). The NMDA antagonist CPPene was in the culture medium during pairing (+CPP, 1 µM, n = 14). In all cumulative frequency plots the non-paired group was added as reference. P values (Kolmogorov-Smirnov) are vs no pairing group. **g,** The median input strength (% no pairing median) plotted relative to the light-induced EPSPs (arrows) and action potential timings (vertical ticks on colored bars) during oSTDP pairing (data from **e,** brown +50 ms, violet -50 ms, cyan -10 ms, magenta +10 ms). Two cycles (of 300) at 5 Hz are illustrated.

As for STDP[2,3,24,25,28], tLTP induced in the incubator was abolished when NMDA receptors were blocked during pairing (Fig. 3f, +CPP). Reducing the pairing frequency from 5 Hz to 0.1 Hz also prevented plasticity induction (Fig. 3f, 0.1 Hz), in line with previous studies[27].

No depression after no-patch oSTDP. It was unexpected that anti-causal pairing of pre- and postsynaptic spikes did not decrease the input strength when assessed 3 hours or 3 days later (Fig. 3d, e). As the stimulation was repeated every 200 ms, the tested timings covered all possible phase shifts between pre- and postsynaptic activity (Fig. 3g). The absence of tLTD was particularly surprising because during patch-clamp recordings, causal and anti-causal oSTDP clearly had opposite effects on EPSCs (Fig. 1g-i). As the distribution of input strengths following anti-causal pairing (-10 ms) appeared rather bimodal, we tested pairing protocols of different length in an attempt to uncover the expected depression[27]. However, while 30 anti-causal pairings at 5 Hz did not induce any plasticity, all stronger protocols (100 to 500 repeats at 5 Hz) increased input strength (Supplementary Fig. 5). Thus, tLTD was observed only at short time points (20 min) during patch-clamp recordings, and was not observed at later time points when the CA1 neurons were not patched during oSTDP induction.

Activity level in the slice is important for long term potentiation. We were intrigued that the strength of causally paired CA3-CA1 connections seemed to increase in the days following plasticity induction, since no additional external stimulation was provided during the incubation period. We reasoned that after oSTDP, circuits containing potentiated synapses might develop higher levels of spontaneous spiking in the incubator, increasing re-activation of the synapses between the paired CA3 and CA1 neurons[35,36]. We either globally disturbed activity by completely changing the slice culture medium 3-4 hours after oSTDP or suppressed activity by including tetrodotoxin in the fresh medium. Both manipulations prevented potentiation of the synapses from ChrimsonR-CA3 to

197 CheRiff-CA1 neurons (Fig 4). These experiments indicate that the synaptic memory of a short episode
198 of coincident activity was actively maintained and amplified in the cultures, pointing to a process that
199 requires replay of activity patterns in the selected circuits.

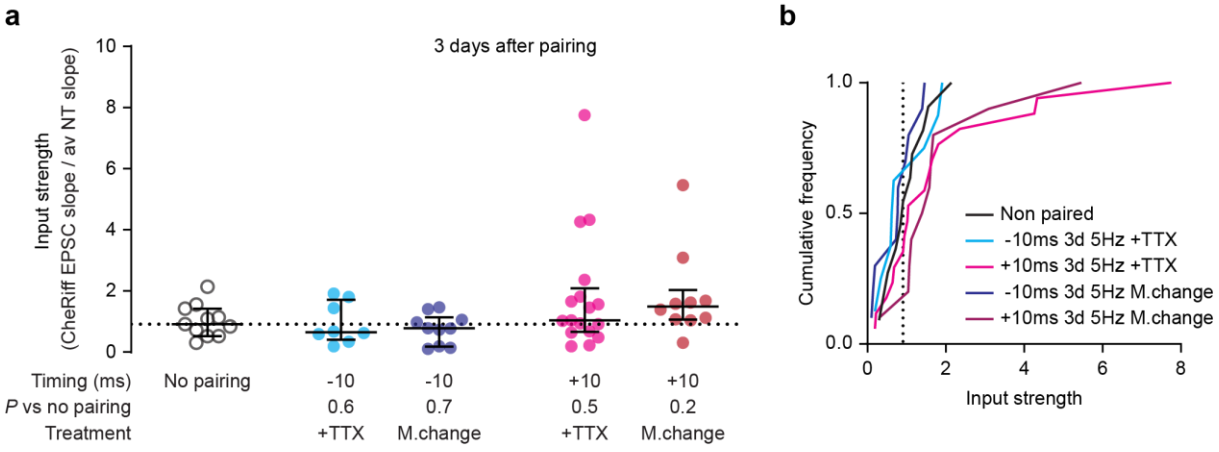

200

201 **Fig. 4 | Activity in the paired pathway is essential for long term potentiation. a,** Normalized input strength of
202 CheRiff-CA1 neurons recorded from causally or anti-causally (300 rep at 5 Hz) paired slices 3 days later. The no
203 pairing group is reproduced from **Fig 3d**. Three to four hours after oSTDP medium was changed (M change) to
204 increase global activity or activity was blocked with tetrodotoxin (+TTX, 1 µM). Two days later medium was
205 changed again and TTX washed off (n's left to right = 11, 8, 10, 17, 10). Plotted are individual data points,
206 median and 25-75% interquartile range. P values (Kolmogorov-Smirnov) are vs no pairing group. **b,** Cumulative
207 frequency distributions of **a**.

208 **Discussion**

209 By independently activating pre- and postsynaptic neurons with light, we observed that the
210 relationship between spike-EPSP timing and the direction of synaptic plasticity is different at short
211 (20 min) and long (3 day) timescales. Whereas at short time scales, anti-causal and causal pairing
212 respectively depressed and potentiated synapses, three days later synapses were potentiated
213 regardless of the ~10 ms pairing order. Late oSTDP still has a strong dependence on timing as when
214 the EPSP preceded the APs by 50 ms, no plasticity was induced. The requirement for active NMDA
215 receptors during the pairing suggests that elevated intracellular [Ca^{2+}] in the postsynaptic neurons
216 was an essential part of the induction process as has been demonstrated for 'classical' short term
217 STDP[24]. In addition, late oSTDP exhibited similar frequency-dependence to that reported for the CA3-
218 CA1 synapses used in this study[27]. At a pairing repetition rate of 5 Hz tLTP was observed, but not
219 when the pairing rate was reduced to 0.1 Hz.

220 We chose the 3 day time point for our long-term readout because it allowed us to exchange the slice
221 culture medium for the last time 24-48 hours before oSTDP induction and avoid disturbing the
222 cultures before the readout. In addition to the time of the readout, there are other methodological
223 differences between our observations 20 min and 3 days after oSTDP that should be considered. The
224 data obtained 20 min after oSTDP were from individual whole-cell recordings and synaptic strength

post-pairing was compared to the strength at baseline. Three days later, the reference was not to baseline but to neighboring neurons. Potentiation would be apparent either if the synapses onto the CheRiff-CA1 neurons became stronger or if the synapses onto the non-transfected neurons weakened. Although we cannot rule out the second explanation, we favor the first. Another important difference is that in the short term experiments the postsynaptic neurons were recorded from with whole-cell patch-clamp electrodes. Care was taken to begin the oSTDP induction within 10 minutes of obtaining whole-cell access as it is well-known that washout of important cellular components can prevent plasticity[37]. STDP studies using sharp electrodes or perforated patch recordings, which minimize washout of intracellular contents, have reported both tLTD and tLTP but cannot rule out an effect of the recordings per se[38,39]. Thus, the act of patching the postsynaptic neurons during induction with the partial washout of cellular contents might artificially uncover tLTD.

Because of the time it takes to transfer and settle a slice in the recording chamber and to record EPSCs from the minimum four neurons per slice, we could not obtain data after stimulating in the incubator sooner than 1-3 hours after oSTDP. At this earliest obtainable time point after no-patch oSTDP, there was no statistically significant difference in synaptic input onto the CheRiff-CA1 neurons. The variability of synaptic inputs from the ChrimsonR-CA3 neurons might be too large to allow detection of a modest increase in synaptic strength at this early time point. Ongoing reactivation of these synapses during the following days appears necessary to increase sufficiently their strength relative to their neighbors for the potentiation to be detectable. Although there is spontaneous activity in slice cultures, strongly increasing the overall activity shortly after oSTDP prevented the potentiation, as did blocking all activity. We hypothesize that slight differences in synaptic strength, induced by the only structured input that was ever provided in these slice cultures, were enhanced by a process akin to overfitting. In the future, it will be interesting to test this hypothesis by challenging the system with a series of different activation patterns, which will require a more sophisticated illumination system inside the incubator.

The majority of STDP studies report both potentiation and depression. 'LTP-only' STDP windows have however, been observed at human hippocampal, human and rat neocortical synapses[40,41] and in mouse hippocampus[27], most commonly in the presence of increased dopamine[39,42]. If presynaptic activity is paired with prolonged postsynaptic bursts (plateau potentials), the timing window for Schaffer collateral potentiation can be extended to several seconds in the causal and anti-causal direction[43]. Explanations for these discrepant observations abound, but we speculate that if synaptic strength was assessed after several days, the outcome of repeated coincident activity may always be potentiation regardless of the exact temporal sequence. Conservation of total synaptic weight may be provided by heterosynaptic LTD or via generalized downscaling processes[44], e.g. during sleep[45,46].

An alternative strategy to temporally separate plasticity induction and read-out is the use of 'chemical' LTP or LTD protocols. However, any attempt to potentiate (or depress) *all* synapses in the tissue is bound to engage powerful homeostatic mechanisms to re-establish physiological levels of excitation. Here we specifically induce plasticity at a small subset of synapses and can therefore distinguish between plasticity-induced changes and homeostatic changes that might occur at neighboring synapses.

In our experiments, we paired pre- and postsynaptic activity in about 30 ChrimsonR-CA3 neurons and 1-5 CheRiff-CA1 neurons. The increased input strength three days after oSTDP induction might reflect an increase in postsynaptic excitability, an increase in the size and strength of individual pre-existing synapses, an increase in the number of synaptic contacts, or a combination. There was no evidence that a lasting change in excitability of the postsynaptic neuron accounts for the observed increase in input strength[33–35], as there were no differences in the passive and active membrane parameters measured in the CheRiff- and non-transfected CA1 neurons (Supplementary Fig. 4). By extending the observation time window from minutes to days, oSTDP could be combined with additional techniques, such as repeated single spine calcium[8], voltage or sodium imaging[47], or serial electron microscopy[48,49] to determine whether the number or the strength of synapses is changing.

Methods

Rat organotypic hippocampal slice cultures

Wistar rats were housed and bred at the University Medical Center Hamburg-Eppendorf (UKE) animal facility and sacrificed according to German Law (Tierschutzgesetz der Bundesrepublik Deutschland, TierSchG) with approval from the Behörde für Gesundheit und Verbraucherschutz Hamburg and the animal care committee of the UKE. The procedure for organotypic cultures was modified from Stoppini et al.[50], using media without antibiotics[51]. Hippocampi were dissected from P5-P7 pups, cut into 400 µm thick slices using a tissue chopper (McIlwain) and cultured on 30 mm membrane inserts (Millicell Cell Culture Insert, pore size 0.4 µm; PICM0RG50) at 37°C with 5% CO_2. Culture medium contained 79% minimum essential medium (MEM, Sigma; M7278), 20% heat-inactivated horse serum (Gibco; 16050122), D-glucose (13 mM, Fluka; 49152), NaCl (109 mM, Sigma; S5150-1L), $MgSO_4$ (0.8 mM, Fluka; 63126-1L), $CaCl_2$ (1.8 mM, Fluka; 21114-1L), L-glutamine (1 mM, Gibco; 25030-024), insulin (0.01 mg ml^{-1}, Sigma; I6634), ascorbic acid (6 µM, Fluka; 11140), pH 7.28, 320 mOsm kg^{-1}. After opsins were expressing, great care was taken to protect the cultures from wavelengths of light below 560 nm to prevent unintentional co-activation of ChrimsonR and CheRiff-expressing neurons. Handling and normal medium changes (2/3, twice per week) were under dim

291 yellow light, which may directly depolarize ChrimsonR but not CheRiff expressing neurons (Osram
292 LUMILUX CHIP control T8).

293 **Viral vector-based transduction**

294 The plasmid pAAV-syn-ChrimsonR-TdTomato, a kind gift from Edward Boyden (Addgene # 59171),
295 was packaged into AAV viral particles with serotype Rh10 ($7.22*10^{13}$ vg ml^{-1}) at the Vector Core
296 facility of the University Medical Center Hamburg-Eppendorf. One µl was loaded into a micropipette
297 with the tip broken to ~10 µm diameter. Slice cultures (12-14 DIV) were transferred into sterile pre-
298 warmed (37 °C) HEPES-buffered solution containing: NaCl (145 mM, Sigma; S5886-500G), HEPES (10
299 mM, Sigma; H4034-100G), D-glucose (25 mM, Sigma; G7528-250G), KCl (2.5 mM, Fluka; 60121-1L),
300 $MgCl_2$ (1 mM, Fluka; 63020-1L), $CaCl_2$ (2 mM, Honeywell; 21114-1L), pH 7.4, 318 mOsm kg^{-1}. The
301 virus-containing pipette was inserted into CA3 and a small bolus was pressure-ejected using 3-5
302 pressure pulses (Picospritzer: 2 bar, 80-100 ms). Our aim was to transduce approximately 30 CA3
303 neurons in CA3 with ChrimsonR. A detailed description of the viral transduction has been published[52].

304 **Single-cell electroporation**

305 Plasmids used for electroporation were: 1) pAAV-hsyn-CheRiff-eGFP (Addgene #51697), 0.5 ng ml^{-1},
306 kindly provided by Adam Cohen; 2) pCI-syn-mKate2, 10 ng ml^{-1} was created by replacing GCaMP3 in
307 pCI-syn-GCaMP3[9] using hindIII and NotI with mKate2-N from pmKate2-N (Evrogen cat. # FP182).
308 Plasmids were diluted in intracellular solution containing: K-gluconate (135 mM, Sigma; G4500-
309 100G), EGTA (0.2 mM, Sigma-Aldrich; E0396-10G), HEPES (10 mM, Sigma; H4034-100G), $MgCl_2$ (4
310 mM, Fluka; 63020-1L), Na_2-ATP (4 mM, Aldrich; A26209-1G), Na-GTP (0.4 mM, Sigma; G8877-
311 100MG), Na_2-phosphocreatine (10 mM, Sigma; P7936-1G), ascorbate (3 mM, Sigma; A5960-100G),
312 pH 7.2, 295 mOsm kg^{-1}. Slice cultures were transferred to a sterile microscope chamber filled with
313 sterile 37°C HEPES-buffered solution (see viral vector-based transduction) either right after AAV
314 injection or 1 day later. Pipettes (10-15 MΩ, World Precision Instruments; TW150F-3) were filled with
315 the plasmid mixture and several pyramidal neurons in CA1 were touched and electroporated using
316 an Axoporator (25 pulses, -12 V, 500 µs, 50 Hz). A detailed description of the electroporation
317 procedure has been published[53].

318 **CheRiff and ChrimsonR characterization**

319 For characterizing responses to multiple wavelengths, we used a pE-4000 CoolLED (CoolLED Ltd., s/n
320 CP0180) with an additional filter for 550 nm (555±20 nm) coupled through the dual camera port of
321 the electrophysiology setup described below. Light intensities in the specimen plane were measured
322 using a 918D-ST-UV sensor and 1936R power meter (Newport). Light flashes (2 ms, low to high
323 intensity) were delivered every 20s with one minute between wavelength sequences. Whole cell
324 currents were recorded (see electrophysiology below) with synaptic transmission and action

325 potentials blocked by CPPene (10 µM, Tocris bioscience; 1265), NBQX (10 µM, Tocris bioscience;
326 1044), picrotoxin (100 µM, Sigma; P1675-1G) and tetrodotoxin (1 µM, HelloBio; HB1035). Seven CA1
327 (CheRiff) and eleven CA3 (ChrimsonR) neurons were recorded from to obtain n = 4 responses at each
328 wavelength/intensity combination. Average peak light-evoked currents were determined and plotted
329 (Supplementary Fig. 1) using a self-written MATLAB code.

330 **Electrophysiology and optogenetic stimulation**

331 The setup was based on an Olympus BX61WI microscope fitted with Dodt contrast, epifluorescence
332 and CCD-camera (DMK23U274, The Imaging Source) on a dual camera port (see Fig. 1.e). For light
333 stimulation through the objective an LED combiner (Mightex Systems, wavelengths 625, 530, 470,
334 405 nm) was coupled via 1 mm multimode fiber and collimator (Thorlabs) mounted on one of the
335 camera ports. A 40x water immersion objective (Plan-Apochromat 1.0 NA DIC VIS-IR, Zeiss,
336 illuminated field ø 557 µm) or a 10x water immersion objective (UMPlanFL 0.30 NA W, Olympus,
337 illuminated field ø 2.65 mm) were used. Light intensities through the objectives were measured in
338 the specimen plane using a calibrated power meter (LaserCheck, Coherent or 918D-ST-UV sensor /
339 1936R power meter, Newport). To locally activate CA3 neurons, the orange (594) laser beam of an
340 Omicron Light Hub was coupled to an optical fiber fitted with a collimator (Thorlabs) mounted on a
341 lockable swing arm. This construction allowed us to point the laser beam at different angles through
342 the center of the back aperture of the oil immersion condenser (NA 1.4, Olympus) to locally
343 illuminate neurons in CA3 away (~1.5 mm) from the optical axis, with high intensity and little light
344 scattering (Fig 1e). After final laser positioning, the stage was not moved and CA1 neurons within the
345 single field of view were recorded from.

346 Whole-cell patch-clamp recordings were performed using an Axopatch 200B (Axon Instruments, Inc.)
347 amplifier, National Instruments A/D boards and Ephus software[54]. All recordings, except the
348 experiments in Fig. 1g-i and 2b-d (see next section), were performed blind to slice treatment at 30°C
349 (in-line heater, Warner Instruments) in artificial cerebral spinal fluid containing: NaCl (119 mM,
350 Sigma; S5886-500G), $NaHCO_3$ (26.2 mM, Sigma; S5761-500G), D-glucose (11 mM, Sigma; G7528-
351 250G), KCl (2.5 mM, Fluka; 60121-1L), NaH_2PO_4 (1 mM, Sigma; S5011-100G), $MgCl_2$ (4 mM, Fluka;
352 63020-1L), $CaCl_2$ (4 mM, Honeywell; 21114-1L), pH 7.4, ~310 mOsm kg^{-1}, saturated with humidified
353 95% O_2 / 5% CO_2. Patch electrodes (3-4 MΩ, World Precision Instruments; 1B150F-3) were filled with
354 the same intracellular solution used for electroporation (above). Liquid junction potential was
355 measured (-14.1 to -14.4 mV) and corrected. CA1 pyramidal neurons were patched under the 40x
356 water immersion objective and voltage-clamped at -70 mV (LJP corrected). A test pulse (-5 mV, 200
357 ms) was applied at the start of every sweep. Series resistance (Rs) was less than 20 MΩ, did not

358 change more than 30% and was not compensated in voltage clamp. In current clamp we used the
359 bridge balance compensation.

360 **Optogenetic induction of spike-timing dependent plasticity during whole-cell recordings**

361 Eight to eleven days after virus injection and electroporation of ChrimsonR and CheRiff, slices were
362 transferred to the electrophysiology setup and perfused with slice culture medium (described above)
363 without horse serum (replaced with MEM), supplemented with D-serine (30 µM, Tocris Bioscience;
364 0226) and diluted slightly to give ~308 mOsm kg^{-1} (33 °C, saturated with humidified 95% O_2 / 5% CO_2).
365 The liquid junction potential was measured and corrected (-15.3 mV). The medium (50 ml) was
366 recycled during the experiment and changed every 3 hours or every 3 slices, whichever came first.
367 With the 594 nm laser positioned to stimulate ChrimsonR-CA3 neurons, a CA1 neuron was patched
368 and EPSCs were recorded (every 20s) at -65.3 mV (LJP corrected) where inhibitory currents were
369 clearly outward. Laser intensity was set to evoke EPSCs of approximately -100 pA (range -50 pA to -
370 200 pA). Baseline EPSCs were recorded for up to 5 minutes after break-in. The 10x objective was
371 carefully moved into position to maximize the area of the slice illuminated and the amplifier was
372 switched to current clamp to allow spiking of the CA1 neuron during paired optogenetic stimulation.
373 To induce plasticity, stimulation of ChrimsonR-CA3 neurons 300 x 2 ms pulses at 5 Hz (594 nm laser
374 at baseline intensity plus simultaneous red LED stimulation in the CA1 (625 nm, 2 mW mm^{-2})) was
375 combined with bursts of 3 violet LED stimuli in CA1 (405 nm, 2 ms, 50 Hz, 1 mW mm^{-2}) to activate
376 CheRiff-CA1 neurons. We set the delay between orange/red and the last or first of the violet light
377 flashes of -10 ms or +10 ms for anti-causal and causal pairing, respectively but after 9 experiments
378 observed the actual median delay from the last action potential (AP) to EPSP onset was -14.2 ms
379 during anti-causal pairing and from EPSP onset to the first AP was 6.8 ms during causal pairing. We
380 therefore advanced the red/orange flash by 2 ms relative to the violet flash during the remaining
381 experiments obtaining a more symmetrical median timing of -12.4 ms during anti-causal and 8.8 ms
382 during causal pairing. After pairing CA3 and CA1 stimulation, EPSCs (0.05 Hz orange laser flashes)
383 were recorded for an additional 25 minutes. The EPSC slope was measured using a self-written script
384 in MATLAB. To determine whether tLTP or tLTD occurred in an individual experiment the baseline
385 slopes (black points in Fig. 1g) and the slopes measured in the last 5 minutes (magenta points in Fig.
386 1g) were compared with Kolmogorov-Smirnov tests (significance $p < 0.05$). A Kolmogorov-Smirnov
387 test was used to test whether the normalized EPSC slopes were different between the anti-causal
388 and causally paired groups. Plots and statistical analyses were performed using GraphPad Prism.

389 **In-incubator oSTDP, read-out and analysis**

390 For all 'no patch' oSTDP experiments, read-out and analysis were performed by an investigator (MA
391 or BvB) blinded to the induction protocol. Unblinding occurred after the target n for a particular

392 group was reached (~ 7 CheRiff neurons from 4 slices). Experimental groups were inter-mixed to
393 ensure blinding and to mitigate the possibility of unexpected batch or time-dependent factors
394 influencing the outcome resulting in uneven n's between treatment groups.

395 We waited 7-10 days to allow stable expression of ChrimsonR and CheRiff. One to three days before
396 in-incubator light stimulation, the slice cultures (placed singly on the inserts) were transferred to and
397 centered in a 35 mm culture dish. Where indicated CPPene (1 µM, Fig. 3) was added to the slice
398 culture medium the day before. The closed petri dish containing the centered slice culture was
399 placed in an LED illumination tower constructed from 30 mm optical bench parts (Thorlabs) that was
400 inside a dedicated incubator (Fig. 2a). The tower contained an injection-molded reflector (Roithner
401 LaserTechnik, 10034) to collimate the 630 nm LED (Cree XP-E red) and an aspheric condenser lens
402 (Thorlabs ACL2520U-A) to collimate the 405 nm LED (Roschwege Star-UV405-03-00-00). The LEDs
403 were powered and controlled from outside the incubator by a two-channel Grass S8800 stimulator,
404 two constant-current drivers (RECOM RCD-24-1.20) and a timer. LED power was adjusted to give 1.2
405 mW mm^{-2} for 405 nm and 8 mW mm^{-2} for 630 nm inside the petri dish in the specimen plane.
406 Considering the spread in actual spike-burst delay (Fig. 1i), Δt was set to +52, +12, -8, or -48 ms to
407 produce EPSP-spike delays of ~+50 ms, +10 ms, -10 ms and -50 ms, respectively (light pulse duration
408 2 ms). Pairing frequency was 5 Hz or 0.1 Hz. Paired activation was repeated 300 times unless
409 otherwise indicated. 'Non-paired' cultures were handled identically but no light stimulation was
410 given. After pairing, each petri dish was marked with only a letter code and date/time of pairing.
411 Where indicated (Fig. 4), 3-4 hours after pairing fresh pre-warmed medium with 1 µM tetrodotoxin
412 (TTX) was pipetted on top of the membrane to immediately silence neurons in the slice. The medium
413 under the slice was then aspirated, replaced with the TTX containing medium and the medium on top
414 of the slice was removed before returning the slice to the incubator, so that the slice was again
415 exposed to the humidified incubator atmosphere. Two days later the TTX was washed 3x and the
416 slices returned to the incubator until the following day when they were recorded from. For the
417 medium change condition, cultures were handled identically except the medium never contained
418 TTX.

419 One hour or 3 days after in-incubator stimulation, slices were transferred by the blinded investigator
420 to the electrophysiology setup with on/off axis stimulation and perfused with ACSF at 30 °C as
421 described above. The slice was positioned so that CheRiff-CA1 neurons as well as at least 5 non-
422 transfected CA1 pyramidal neurons were in the field of view of the 40x objective and camera (Fig.
423 3a). The 594 nm laser was positioned to activate the ChrimsonR-CA3 neurons (see above). Whole-cell
424 patch-clamp recordings were sequentially made from 3 to 4 non-transfected CA1 pyramidal neurons
425 and 1 to 5 CheRiff-CA1 pyramidal neurons in a pseudo-random sequence without moving the stage
426 to ensure constant CA3 stimulation (holding potential -70 mV to ensure separation between EPSCs

427 and IPSCs). While still in cell-attached mode, each neuron was illuminated with a single 405 nm light
428 flash (1 ms, 1.2 mW mm^{-2}) to double-check if the neuron was non-transfected (no spike) or CheRiff-
429 expressing (light-induced spike). After break-in, orange laser flashes (594 nm, 20 s interval)
430 stimulated ChrimsonR-CA3 neurons to evoke EPSCs in the CA1 neurons. EPSC onset was typically 6 to
431 8 ms after the stimulation. If the delay to EPSC onset was 13 ms or longer they were assumed
432 polysynaptic and not analyzed. Ten EPSCs were recorded at each of 3 laser intensities from each CA1
433 neuron (when spontaneous events obscured the EPSCs a few more sweeps were collected). The
434 middle intensity was set to evoke an EPSC of about -100 to -300 pA in the first recording from a given
435 slice. The same 3 intensities were used for all neurons in a given slice. At the end of each recording,
436 we injected a series of current steps to assess cellular excitability. Cells without pyramidal-like firing
437 patterns (i.e. high AP frequency, large amplitude after-hyperpolarization) were eliminated from the
438 analysis.

439 For analysis, we selected the EPSCs from one laser intensity per slice. The selected intensity evoked
440 the most similar EPSC slopes that were at least 20 pA in three non-transfected cells (usually the
441 lowest laser intensity). Individual sweeps with spontaneous EPSCs/IPSCs within 10 ms of the
442 stimulation were suppressed. If fewer than 4 sweeps remained at the selected laser intensity, the
443 recording was discarded. A custom MATLAB routine averaged the EPSCs, detected the (first) peak
444 and the 20-60% slope (Fig. 3c). If the time of the peak varied by more than 5 ms between neurons,
445 we suspected a mixture of mono and polysynaptic responses and the slice was excluded. Input
446 strength we define as the slope from each CheRiff-CA1 neuron divided by the slope of the average
447 EPSC from all non-transfected neurons. GraphPad Prism 8 was used for statistics and to create plots.

448 **Immunohistochemistry**

449 Ninety minutes after stimulation, slices were fixed (30 minutes, ice-cold 4% paraformaldehyde in
450 PBS). Slices were washed in PBS (3 x 10 min) and blocked (2 hours 5% donor horse serum, 0.3 %
451 Triton™ X-100 in PBS at RT). Slices were incubated overnight with the primary antibody (4° C, rabbit
452 anti-cFos, Santa Cruz Biotechnology, Inc., sc-52, 1:500) in carrier solution (1 % Bovine serum albumin,
453 0.3 % Triton™ X-100 in PBS), then washed 3 times in PBS and incubated at RT for 2 hours with a
454 secondary antibody (Alexa Fluor 488 goat anti-rabbit, Life Technologies, A11008; or Alexa Fluor 568
455 goat anti-rabbit, Life Technologies, A11011) at 1:1000 in carrier solution (same as above). Slices were
456 washed (3 x 10 min) in PBS and mounted with Shandon Immu-Mount (Thermo Scientific; 9990402).

457 For STED microscopy CheRiff-GFP was co-electroporated with 10 ng ml^{-1} pEGFP-N1 (Clontech, #6085-
458 1) instead of the mKate2. Nine days after virus injection/electroporation the slices were fixed and
459 blocked as above. Slices were incubated overnight at 4 °C with primary antibodies (FluoTag-X4 anti-
460 GFP Atto647N, NanoTag, N0304-At647N and FluoTag-Q anti-RFP AbberiorStar580, NanoTag, N0401-

461 Ab580, both at 1:250) in carrier solution. Slices were washed (3 x 10 min in PBS) and mounted in
462 Mowiol 4-88 (Roth 0713.2) prepared according to manufacturer's protocol with DABCO (Sigma-
463 Aldrich, D27802).

464 **Confocal microscopy**

465 An Olympus F1000 confocal microscope and 20x objective (UPLSAPO 0.85 NA, Olympus) were used
466 using the laser/filter sets designed for Alexa 488, Alexa 546 and Alexa 568 as appropriate. Z-series
467 images were obtained using a 3 µm z-step at a 1024x1024-pixel resolution scanning at 12.5 µs per
468 pixel. Image parameters were adjusted for the red and green channels and were kept constant
469 throughout. Fiji/ImageJ[55] was used to project the z-series and overlay channels.

470 **STED microscopy**

471 Gated-2D-STED images were acquired using an Abberior expert-line STED microscope (Abberior
472 instruments). The microscope was controlled by Abberior Inspector software. Samples were placed
473 on a Nikon TI microscope body, equipped with a 60x objective (P-Apo 1.4NA, Nikon). At first,
474 fluorophores were excited with 561 nm and 640 nm laser lines. Both channels, red and far-red were
475 acquired in confocal. In addition, the far-red channel was resolved with 2D-STED by use of a 775nm
476 depletion laser. For both, confocal and 2D-STED acquisitions the pinhole was set to 1AU.
477 Fluorescence was collected on avalanche photodetectors through emission filters 615/20 (red
478 channel) and 685/70 (far-red channel). Gating was obtained with a SPC150 TCSPC board (Becker &
479 Hickl). Gates were set to 8 ns width, starting with a delay of 781.3 ps for both confocal and STED.
480 Acquisitions were obtained sequentially with a 20- by 20 nm pixel size. Confocal images were the
481 result of 6 accumulations, STED images of 18 accumulations acquired by line-mode. Files were saved
482 in a 16-bit format. Confocal and STED images were merged in ImageJ. For representation, the lookup
483 table is linearly adjusted for each channel.

References

1. Song, S., Miller, K. D. & Abbott, L. F. Competitive Hebbian learning through spike-timing-dependent synaptic plasticity. *Nat. Neurosci.* **3**, 919–926 (2000).

2. Debanne, D., Gähwiler, B. H. & Thompson, S. M. Long-term synaptic plasticity between pairs of individual CA3 pyramidal cells in rat hippocampal slice cultures. *J. Physiol.* **507 (Pt 1**, 237–47 (1998).

3. Bi, G. Q. & Poo, M. M. Synaptic modifications in cultured hippocampal neurons: dependence on spike timing, synaptic strength, and postsynaptic cell type. *J Neurosci* **18**, 10464–10472 (1998).

4. Markram, H., Lübke, J., Frotscher, M. & Sakmann, B. Regulation of synaptic efficacy by coincidence of postsynaptic APs and EPSPs. *Science (80-.).* **275**, 213–215 (1997).

5. Gerstner, W., Kempter, R., van Hemmen, J. L. & Wagner, H. A neuronal learning rule for sub-millisecond temporal coding. *Nature* **383**, 76–81 (1996).

6. Costa, R. P., Froemke, R. C., Sjöström, P. J. & van Rossum, M. C. W. Unified pre- and postsynaptic long-term plasticity enables reliable and flexible learning. *Elife* (2015). doi:10.7554/eLife.09457

7. van Rossum, M. C., Bi, G. Q. & Turrigiano, G. G. Stable Hebbian learning from spike timing-dependent plasticity. *J. Neurosci.* **20**, 8812–21 (2000).

8. Wiegert, J. S., Pulin, M., Gee, C. E. & Oertner, T. G. The fate of hippocampal synapses depends on the sequence of plasticity-inducing events. *Elife* **7**, (2018).

9. Wiegert, J. S. & Oertner, T. G. Long-term depression triggers the selective elimination of weakly integrated synapses. *Proc. Natl. Acad. Sci. U. S. A.* **110**, E4510–E4519 (2013).

10. Nagel, G. *et al.* Channelrhodopsin-2, a directly light-gated cation-selective membrane channel. *Proc. Natl. Acad. Sci.* **100**, 13940–13945 (2003).

11. Boyden, E. S., Zhang, F., Bamberg, E., Nagel, G. & Deisseroth, K. Millisecond-timescale, genetically targeted optical control of neural activity. *Nat. Neurosci.* **8**, 1263–1268 (2005).

12. Zhang, F., Wang, L. P., Boyden, E. S. & Deisseroth, K. Channelrhodopsin-2 and optical control of excitable cells. *Nat Methods* **3**, 785–792 (2006).

13. Zhang, Y.-P. & Oertner, T. G. Optical induction of synaptic plasticity using a light-sensitive channel. *Nat. Methods* **4**, 139–41 (2007).

14. Huber, D. *et al.* Sparse optical microstimulation in barrel cortex drives learned behaviour in freely moving mice. *Nature* **451**, 61–4 (2008).

15. Adamantidis, A. R., Zhang, F., Aravanis, A. M., Deisseroth, K. & de Lecea, L. Neural substrates of awakening probed with optogenetic control of hypocretin neurons. *Nature* **450**, 420–424 (2007).

16. Li, X. *et al.* Fast noninvasive activation and inhibition of neural and network activity by vertebrate rhodopsin and green algae channelrhodopsin. *Proc. Natl. Acad. Sci. U. S. A.* **102**, 17816–21 (2005).

17. Vetere, G. *et al.* Spine growth in the anterior cingulate cortex is necessary for the consolidation of contextual fear memory. *Proc. Natl. Acad. Sci. U. S. A.* **108**, 8456–60 (2011).

18. Schroll, C. *et al.* Light-induced activation of distinct modulatory neurons triggers appetitive or aversive learning in Drosophila larvae. *Curr. Biol.* **16**, 1741–7 (2006).

19. Hochbaum, D. R. *et al.* All-optical electrophysiology in mammalian neurons using engineered microbial rhodopsins. *Nat. Methods* **11**, 825–833 (2014).

20. Klapoetke, N. C. *et al.* Independent optical excitation of distinct neural populations. *Nat. Methods* **11**, 338–46 (2014).

21. Wietek, J. *et al.* Conversion of channelrhodopsin into a light-gated chloride channel. *Science* **344**, 409–412 (2014).

22. Govorunova, E. G., Sineshchekov, O. A., Janz, R., Liu, X. & Spudich, J. L. NEUROSCIENCE. Natural light-gated anion channels: A family of microbial rhodopsins for advanced optogenetics. *Science (80-.).* **349**, (2015).

23. Mager, T. *et al.* High frequency neural spiking and auditory signaling by ultrafast red-shifted optogenetics. *Nat. Commun.* **9**, 1750 (2018).

24. Nevian, T. & Sakmann, B. Spine Ca2+ Signaling in Spike-Timing-Dependent Plasticity. *J. Neurosci.* **26**, 11001–11013 (2006).

25. Tigaret, C. M., Olivo, V., Sadowski, J. H. L. P., Ashby, M. C. & Mellor, J. R. Coordinated activation of distinct Ca2+ sources and metabotropic glutamate receptors encodes Hebbian synaptic plasticity. *Nat. Commun.* **7**, 10289 (2016).

26. Wiegert, J. S., Gee, C. E. & Oertner, T. G. Stimulating neurons with heterologously expressed light-gated ion channels. *Cold Spring Harb. Protoc.* **2017**, 85–91 (2017).

27. Wittenberg, G. M. & Wang, S. S. Malleability of spike-timing-dependent plasticity at the CA3-CA1 synapse. *J Neurosci* **26**, 6610–6617 (2006).

28. Holbro, N., Grunditz, A., Wiegert, J. S. & Oertner, T. G. AMPA receptors gate spine Ca(2+) transients and spike-timing-dependent potentiation. *Proc Natl Acad Sci U S A* **107**, 15975–15980 (2010).

29. Edelmann, E. *et al.* Theta Burst Firing Recruits BDNF Release and Signaling in Postsynaptic CA1 Neurons in Spike-Timing-Dependent LTP. *Neuron* **86**, 1041–1054 (2015).

30. Frey, M. C., Sprengel, R. & Nevian, T. Activity pattern-dependent long-term potentiation in neocortex and hippocampus of GluA1 (GluR-A) subunit-deficient mice. *J Neurosci* **29**, 5587–5596 (2009).

31. Debanne, D., Gahwiler, B. H. & Thompson, S. M. Heterogeneity of synaptic plasticity at unitary CA3-CA1 and CA3-CA3 connections in rat hippocampal slice cultures. *J Neurosci* **19**, 10664–10671 (1999).

32. Schoenenberger, P., Gerosa, D. & Oertner, T. G. Temporal control of immediate early gene induction by light. *PLoS One* **4**, e8185 (2009).

33. Frick, A., Magee, J. & Johnston, D. LTP is accompanied by an enhanced local excitability of pyramidal neuron dendrites. *Nat. Neurosci.* **7**, 126–135 (2004).

34. Debanne, D. & Poo, M.-M. Spike-timing dependent plasticity beyond synapse - pre- and post-synaptic plasticity of intrinsic neuronal excitability. *Front. Synaptic Neurosci.* **2**, 21 (2010).

35. Debanne, D., Inglebert, Y. & Russier, M. Plasticity of intrinsic neuronal excitability. *Curr. Opin.*

Neurobiol. **54**, 73–82 (2019).

36. Sadowski, J. H. L. P., Jones, M. W. & Mellor, J. R. Sharp-Wave Ripples Orchestrate the Induction of Synaptic Plasticity during Reactivation of Place Cell Firing Patterns in the Hippocampus. *Cell Rep.* **14**, 1916–1929 (2016).

37. Malinow, R. & Tsien, R. W. Presynaptic enhancement shown by whole-cell recordings of long-term potentiation in hippocampal slices. *Nature* **346**, 177–180 (1990).

38. Meredith, R. M., Floyer-Lea, A. M. & Paulsen, O. Maturation of long-term potentiation induction rules in rodent hippocampus: role of GABAergic inhibition. *J. Neurosci.* **23**, 11142–6 (2003).

39. Zhang, J.-C., Lau, P.-M. & Bi, G.-Q. Gain in sensitivity and loss in temporal contrast of STDP by dopaminergic modulation at hippocampal synapses. *Proc. Natl. Acad. Sci. U. S. A.* **106**, 13028–33 (2009).

40. Testa-Silva, G. Human synapses show a wide temporal window for spike-timing-dependent plasticity. *Front. Synaptic Neurosci.* (2010). doi:10.3389/fnsyn.2010.00012

41. Verhoog, M. B. *et al.* Mechanisms underlying the rules for associative plasticity at adult human neocortical synapses. *J. Neurosci.* **33**, 17197–208 (2013).

42. Brzosko, Z., Schultz, W. & Paulsen, O. Retroactive modulation of spike timing-dependent plasticity by dopamine. *Elife* **4**, (2015).

43. Bittner, K. C., Milstein, A. D., Grienberger, C., Romani, S. & Magee, J. C. Behavioral time scale synaptic plasticity underlies CA1 place fields. *Science* **357**, 1033–1036 (2017).

44. Turrigiano, G. G. The dialectic of Hebb and homeostasis. *Philos. Trans. R. Soc. B Biol. Sci.* **372**, 20160258 (2017).

45. Diering, G. H. *et al.* Homer1a drives homeostatic scaling-down of excitatory synapses during sleep. *Science* **355**, 511–515 (2017).

46. de Vivo, L. *et al.* Ultrastructural evidence for synaptic scaling across the wake/sleep cycle. *Science (80-.).* **355**, (2017).

47. Antic, S. D. *et al.* Voltage imaging to understand connections and functions of neuronal circuits. *J. Neurophysiol.* (2016). doi:10.1152/jn.00226.2016

48. Bourne, J. N., Chirillo, M. A. & Harris, K. M. Presynaptic ultrastructural plasticity along CA3→CA1 axons during long-term potentiation in mature hippocampus. *J. Comp. Neurol.* **521**, 3898–3912 (2013).

49. Maco, B. *et al.* Semiautomated correlative 3D electron microscopy of in vivo–imaged axons and dendrites. *Nat. Protoc.* **9**, 1354–1366 (2014).

50. Stoppini, L., Buchs, P. A. & Muller, D. A simple method for organotypic cultures of nervous tissue. *J. Neurosci. Methods* **37**, 173–82 (1991).

51. Gee, C. E., Ohmert, I., Wiegert, J. S. & Oertner, T. G. Preparation of Slice Cultures from Rodent Hippocampus. *Cold Spring Harb. Protoc.* **2017**, 126–130 (2017).

52. Wiegert, J. S., Gee, C. E. & Oertner, T. G. Viral vector-based transduction of slice cultures. *Cold Spring Harb. Protoc.* **2017**, 131–134 (2017).

53. Wiegert, J. S., Gee, C. E. & Oertner, T. G. Single-Cell Electroporation of Neurons. *Cold Spring Harb. Protoc.* **2017**, 135–138 (2017).

54. Suter, B. A. *et al.* Ephus: multipurpose data acquisition software for neuroscience experiments. *Front. Neural Circuits* **4**, 100 (2010).

55. Schindelin, J. *et al.* Fiji: an open-source platform for biological-image analysis. *Nat. Methods* **9**, 676–682 (2012).

Acknowledgements

We would like to thank Iris Ohmert, Sabine Graf, Torsten Renz, Dirk Lubrich, Lennart Sobirey, Paul Lamothe and Ingke Braren (UKE Vector facility) for important technical support. CheRiff was a gift from Adam Cohen, ChrimsonR was a gift from Edward Boyden. The first spectral characterization of ChrimsonR-expressing neurons in slice cultures was performed by Katie Ferguson and Longzhi Tan during the 2014 Neurobiology Course at MBL in Woods Hole. Funding was received from: the Landesforschungsförderung Hamburg; the Deutsche Forschungsgemeinschaft (DFG) grants SPP 1665 220176618, SPP1926 315380903, SFB 936 178316478, SFB 1328 335447717, FOR 2419 278170285, Emmy Noether 259979908; the European Research Council (ERC-StG 714762).

Author contributions

Conceptualization, CEG, TGO, JSW; **Investigation,** MA, BvB, CEG; **Writing – Original Draft,** CEG, TGO, MA; **Writing – Review and Editing,** CEG, TGO, MA, BvB, JSW, MM; **Technical expertise,** TGO, CEG, MM; **Visualization,** MA, CEG, TGO; **Supervision,** CEG, TGO; **Project Funding Acquisition,** CEG, JSW. All authors approved the author list and final version.

Competing interest statement

All authors declare they have no competing interests.